Brief Paper ACTA AUTOMATICA SINICA Vol. 35, No. 7 July, 2009

Static Anti-windup Synthesis for a Class of Linear Systems Subject to Actuator Amplitude and Rate Saturation

LIU Sheng[1] ZHOU Li-Ming[1]

Abstract For a wide class of linear saturated systems, we address the anti-windup synthesis problem. By absorbing the actuator dynamics into the augmented system, we show that the original system can be simplified to a larger system with only amplitude saturation. The static anti-windup gain is therefore obtained through the proposed linear matrix inequality (LMI) based optimization procedures with regional closed-loop stability and minimized nonlinear L_2 gain. A simulation example illustrates the effectiveness of the approaches.

Key words Static anti-windup, amplitude and rate saturation, linear matrix inequality (LMI)

Linear systems with saturating actuator have attracted much attention for the past decade[1−14]. However, effectively solvable controller synthesis approaches have rarely been established, especially with practically encountered actuator amplitude and rate saturation, such as in reaction processes and ship steering control systems[1−2]. More specifically, most of the works adopted the framework of direct nonlinear design[2−3], whereas the approaches based on the anti-windup framework were preferred, since the design parameters could always be obtained via convex optimization[4−8]. The anti-windup framework, composed of an unconstrained controller and an anti-windup compensator, can fully utilize the mature linear design techniques in synthesizing the former. When the actuator saturates, the anti-windup compensator ensures less performance degradation and stability deterioration. In comparison with the traditional global sectors, the recently proposed generalized sector condition led to less conservative analysis methods[9−10] and more effective controller design techniques using linear matrix inequalities (LMIs) and/or bilinear matrix inequalities (BMIs)[9−14]. Accordingly, Hu introduced the polytopic differential inclusions and the norm-bounded differential inclusions that contain the saturated system and obtained more effective regional analysis tools[12]. Following this direction, we discuss here the static anti-windup problems with neat theoretical results.

Notations. For $\boldsymbol{u} \in \mathbf{R}^m$, the standard vector-valued saturation function is defined as

$$(\mathrm{sat}(\boldsymbol{u}))_i = \begin{cases} u_i, & |u_i| \le 1 \\ \mathrm{sgn}(u_i), & |u_i| > 1 \end{cases}$$

For $\boldsymbol{u} \in \mathbf{R}^m$, there are two norms $||\boldsymbol{u}||_\infty = \max_i |u_i|$ and $||\boldsymbol{u}||_2 = (\int_0^\infty \boldsymbol{u}^{\mathrm{T}}(t)\boldsymbol{u}(t)\mathrm{d}t)^{\frac{1}{2}}$.

$\mathrm{He}X = X + X^{\mathrm{T}}$ where X is a matrix.

Δ_i belongs to the diagonal matrix set with all the diagonal elements being either 0 or 1.

Received November 9, 2007; in revised form December 13, 2008
Supported by National Natural Science Foundation of China (60704004)
1. College of Automation, Harbin Engineering University, Harbin 150001, P. R. China
DOI: 10.3724/SP.J.1004.2009.01003

With a matrix $H \in \mathbf{R}^{m\times n}$, $\mathcal{L}(H)$ is the set $\{\boldsymbol{x} \in \mathbf{R}^n : ||H\boldsymbol{x}||_\infty \le 1\}$.

For a positive definite matrix P, the ellipsoid $\{\boldsymbol{x} \in \mathbf{R}^n : \boldsymbol{x}^{\mathrm{T}} P\boldsymbol{x} \le 1\}$ is denoted as $\mathcal{E}(P)$, for which the following set inclusion condition holds[9−10]

$$\mathcal{E}(Q^{-1}) \subset \mathcal{L}(H) \Leftrightarrow \begin{bmatrix} 1 & \boldsymbol{Y}_l \\ \boldsymbol{Y}_l^{\mathrm{T}} & Q \end{bmatrix} \ge 0, \quad 1 \le l \le m \tag{1}$$

where $\boldsymbol{Y}_l$ is the l-th row of $Y = HQ$.

1 Problem formulation

Consider a class of linear systems

$$\mathcal{P}: \begin{cases} \dot{\boldsymbol{x}}_p &= A_p\boldsymbol{x}_p + B_{pu}\boldsymbol{u}_p + B_{pw}\boldsymbol{w} \\ \boldsymbol{y}_p &= C_{py}\boldsymbol{x}_p + D_{pyu}\boldsymbol{u}_p + D_{pyw}\boldsymbol{w} \\ \boldsymbol{z}_p &= C_{pz}\boldsymbol{x}_p + D_{pzu}\boldsymbol{u}_p + D_{pzw}\boldsymbol{w} \end{cases} \tag{2}$$

with the actuator dynamics given by

$$\mathcal{A}: \begin{cases} \dot{\boldsymbol{\delta}} &= \mathrm{sat}(K_1\boldsymbol{u}_a + K_2\boldsymbol{\delta}) \\ \boldsymbol{y}_a &= \mathrm{sat}(\boldsymbol{\delta}) \end{cases} \tag{3}$$

where $\boldsymbol{x}_p \in \mathbf{R}^n, \boldsymbol{y}_p \in \mathbf{R}^l, \boldsymbol{u}_p \in \mathbf{R}^m, \boldsymbol{w} \in \mathbf{R}^r$, and $\boldsymbol{z}_p \in \mathbf{R}^p$ are, respectively, the state, the measured output, the control input, the exogenous input (reference and disturbance), and the performance output. K_1 and K_2 are diagonal matrices and $\boldsymbol{\delta}, \boldsymbol{u}_a, \boldsymbol{y}_a \in \mathbf{R}^m$ are the internal state, input, and output vectors of the actuator.

Suppose that an unconstrained controller (i.e., neglecting the saturation effect in (3) and under the interconnection $\boldsymbol{y}_c = \boldsymbol{u}_a, \boldsymbol{y}_a = \boldsymbol{u}_p$) has been designed as

$$\mathcal{C}: \begin{cases} \dot{\boldsymbol{x}}_c &= A_c\boldsymbol{x}_c + B_{cy}\boldsymbol{y}_p + B_{cw}\boldsymbol{w} \\ \boldsymbol{y}_c &= C_c\boldsymbol{x}_c \end{cases} \tag{4}$$

with closed-loop stability and desired performance.

In order to deal with the saturation nonlinearity, we rearrange the original system (2) ∼ (4) and design a static anti-windup compensator F as shown in Fig. 1.

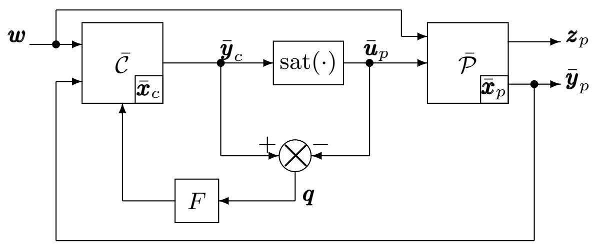

Fig. 1 Closed-loop system with static anti-windup

With the actuator dynamics being absorbed into the augmented plant, the augmented vectors are

$$\begin{cases} \bar{\boldsymbol{x}}_c &= \boldsymbol{x}_c \in \mathbf{R}^{n_c} \\ \bar{\boldsymbol{x}}_p &= (\boldsymbol{x}_p^{\mathrm{T}} \quad \boldsymbol{\delta}^{\mathrm{T}})^{\mathrm{T}} \in \mathbf{R}^{n+m} \\ \bar{\boldsymbol{y}}_c &= (\boldsymbol{\delta}^{\mathrm{T}} \quad \boldsymbol{\eta}^{\mathrm{T}})^{\mathrm{T}} \in \mathbf{R}^{2m} \\ \bar{\boldsymbol{y}}_p &= (\boldsymbol{y}_p^{\mathrm{T}} \quad \boldsymbol{\delta}^{\mathrm{T}})^{\mathrm{T}} \in \mathbf{R}^{l+m} \end{cases}$$

where $\boldsymbol{\eta} = K_1\boldsymbol{u}_a + K_2\boldsymbol{\delta}$ from (3). The anti-windup term $F\boldsymbol{q}$ may enter not only the augmented controller state equation but also the output equation. Clearly, the closed-loop system depicted in Fig. 1 corresponds to the general form in Fig. 2, since the amplitude and rate saturation has been

$$\begin{bmatrix} \bar{A}_c & \bar{B}_{cy} & \bar{B}_{cw} \\ \bar{C}_c & \bar{D}_{cy} & \bar{D}_{cw} \\ & \bar{B}_{c1} & \bar{D}_{c2} \end{bmatrix} = \begin{bmatrix} A_c & B_{cy} & 0 & B_{cw} \\ 0 & 0 & I & 0 \\ K_1 C_c & 0 & K_2 & 0 \\ & I & 0 & \begin{matrix} 0 & 0 \\ 0 & K_1 \end{matrix} \end{bmatrix}, \quad \begin{bmatrix} \bar{A}_p & \bar{B}_{pu} & \bar{B}_{pw} \\ \bar{C}_{py} & \bar{D}_{pyu} & \bar{D}_{pyw} \\ \bar{C}_{pz} & \bar{D}_{pzu} & \bar{D}_{pzw} \end{bmatrix} = \begin{bmatrix} A_p & 0 & B_{pu} & 0 & B_{pw} \\ 0 & 0 & 0 & I & 0 \\ C_{py} & 0 & D_{pyu} & 0 & D_{pyw} \\ 0 & I & 0 & 0 & 0 \\ C_{pz} & 0 & D_{pzu} & 0 & D_{pzw} \end{bmatrix}$$

$$\begin{bmatrix} A & B_q & B_w \\ C_y & D_{yq} & D_{yw} \\ C_z & D_{zq} & D_{zw} \end{bmatrix} = \begin{bmatrix} \bar{A}_p + \bar{B}_{pu}\Delta_u \bar{D}_{cy}\bar{C}_{py} & \bar{B}_{pu}\Delta_u \bar{C}_c & B_1 + B_2 F & \bar{B}_{pw} + \bar{B}_{pu}\Delta_u(\bar{D}_{cw} + \bar{D}_{cy}\bar{D}_{pyw}) \\ \bar{B}_{cy}\Delta_y \bar{C}_{py} & \bar{A}_c + \bar{B}_{cy}\Delta_y \bar{D}_{pyu}\bar{C}_c & & \bar{B}_{cw} + \bar{B}_{cy}\Delta_y(\bar{D}_{pyw} + \bar{D}_{pyu}\bar{D}_{cw}) \\ \bar{D}_{cy}\Delta_y \bar{C}_{py} & \bar{C}_c + \bar{D}_{cy}\Delta_y \bar{D}_{pyu}\bar{C}_c & Y_1 + Y_2 F & \bar{D}_{cw} + \bar{D}_{cy}\Delta_y(\bar{D}_{pyw} + \bar{D}_{pyu}\bar{D}_{cw}) \\ \bar{C}_{pz} + \bar{D}_{pzu}\Delta_u \bar{D}_{cy}\bar{C}_{py} & \bar{D}_{pzu}\Delta_u \bar{C}_c & Z_1 + Z_2 F & \bar{D}_{pzw} + \bar{D}_{pzu}\Delta_u(\bar{D}_{cw} + \bar{D}_{cy}\bar{D}_{pyw}) \end{bmatrix}$$

$$\begin{bmatrix} B_1 & Y_1 & Z_1 & \Delta_u \\ B_2 & Y_2 & Z_2 & \Delta_y \end{bmatrix} = \begin{bmatrix} \begin{matrix} -\bar{B}_{pu}\Delta_u \\ -\bar{B}_{cy}\Delta_y \bar{D}_{pyu} \end{matrix} & -\bar{D}_{cy}\Delta_y \bar{D}_{pyu} & -\bar{D}_{pzu}\Delta_u & (I - \bar{D}_{cy}\bar{D}_{pyu})^{-1} \\ \begin{matrix} \bar{B}_{pu}\Delta_u \bar{D}_{c2} \\ \bar{B}_{c1} + \bar{B}_{cy}\Delta_y \bar{D}_{pyu}\bar{D}_{c2} \end{matrix} & \bar{D}_{c2} + \bar{D}_{cy}\Delta_y \bar{D}_{pyu}\bar{D}_{c2} & \bar{D}_{pzu}\Delta_u \bar{D}_{c2} & (I - \bar{D}_{pyu}\bar{D}_{cy})^{-1} \end{bmatrix}$$

transformed into the standard amplitude saturation. From (2) $\sim$ (4), it is obvious that the corresponding matrices in (5) $\sim$ (7) are uniquely determined by the equations shown at the top of this page.

$$\bar{\mathcal{C}}: \begin{cases} \dot{\bar{\boldsymbol{x}}}_c = \bar{A}_c\bar{\boldsymbol{x}}_c + \bar{B}_{cy}\bar{\boldsymbol{y}}_p + \bar{B}_{cw}\boldsymbol{w} + \bar{B}_{c1}F\boldsymbol{q} \\ \bar{\boldsymbol{y}}_c = \bar{C}_c\bar{\boldsymbol{x}}_c + \bar{D}_{cy}\bar{\boldsymbol{y}}_p + \bar{D}_{cw}\boldsymbol{w} + \bar{D}_{c2}F\boldsymbol{q} \end{cases} \tag{5}$$

$$\bar{\mathcal{P}}: \begin{cases} \dot{\bar{\boldsymbol{x}}}_p = \bar{A}_p\bar{\boldsymbol{x}}_p + \bar{B}_{pu}\bar{\boldsymbol{u}}_p + \bar{B}_{pw}\boldsymbol{w} \\ \bar{\boldsymbol{y}}_p = \bar{C}_{py}\bar{\boldsymbol{x}}_p + \bar{D}_{pyu}\bar{\boldsymbol{u}}_p + \bar{D}_{pyw}\boldsymbol{w} \\ \boldsymbol{z}_p = \bar{C}_{pz}\bar{\boldsymbol{x}}_p + \bar{D}_{pzu}\bar{\boldsymbol{u}}_p + \bar{D}_{pzw}\boldsymbol{w} \end{cases} \tag{6}$$

For a saturated linear system (as depicted in Fig. 2) with the general form

$$\begin{cases} \dot{\boldsymbol{x}} = A\boldsymbol{x} + B_q\boldsymbol{q} + B_w\boldsymbol{w} \\ \boldsymbol{y} = C_y\boldsymbol{x} + D_{yq}\boldsymbol{q} + D_{yw}\boldsymbol{w} \\ \boldsymbol{z} = C_z\boldsymbol{x} + D_{zq}\boldsymbol{q} + D_{zw}\boldsymbol{w} \\ \boldsymbol{q} = \mathrm{dz}(\boldsymbol{y}) \end{cases} \tag{7}$$

where $\boldsymbol{x} \in \mathbf{R}^n, \boldsymbol{q} \in \mathbf{R}^m, \boldsymbol{y} \in \mathbf{R}^m, \boldsymbol{w} \in \mathbf{R}^r, \boldsymbol{z} \in \mathbf{R}^p$, and the vector-valued deadzone function $\mathrm{dz}(\cdot): \mathbf{R}^m \mapsto \mathbf{R}^m$ is defined as $\mathrm{dz}(\boldsymbol{y}) = \boldsymbol{y} - \mathrm{sat}(\boldsymbol{y})$, we assume that the algebraic loop in the second equation of (7) is well-posed. Also note the following:

$$\begin{aligned} T_i &= (I - \Delta_i D_{yq})^{-1}\Delta_i \\ A_i &= A + B_q T_i C_y, \quad B_i = B_w + B_q T_i D_{yw} \\ C_i &= C_z + D_{zq} T_i C_y, \quad D_i = D_{zw} + D_{zq} T_i D_{yw} \end{aligned} \tag{8}$$

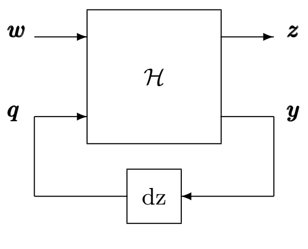

Fig. 2 The general framework of saturated linear systems

2 Main results

Lemma 1[12]**.** Given a matrix $Q \in \mathbf{R}^{n\times n}$, $Q > 0$, and a real positive number γ, let $V(\boldsymbol{x}) = \boldsymbol{x}^{\mathrm{T}}Q^{-1}\boldsymbol{x}$. For system (7), if there exists a matrix $Y \in \mathbf{R}^{m\times n}$ satisfying (1) and

$$\mathrm{He}\begin{bmatrix} A_iQ - B_qT_iY & B_i & 0 \\ 0 & -I/2 & 0 \\ C_iQ - D_{zq}T_iY & D_i & -\gamma^2 I/2 \end{bmatrix} \le 0 \tag{9}$$

then $\dot{V}(\boldsymbol{x},\boldsymbol{w}) + \frac{1}{\gamma^2}\boldsymbol{z}^{\mathrm{T}}\boldsymbol{z} \le \boldsymbol{w}^{\mathrm{T}}\boldsymbol{w}$ for all $\boldsymbol{x} \in \mathcal{E}(Q^{-1})$. Moreover, $\mathcal{E}(Q^{-1})$ is a contractively invariant ellipsoid with $\boldsymbol{w} = 0$ and $||\boldsymbol{z}||_2 \le \gamma||\boldsymbol{w}||_2$ for $\boldsymbol{x}(0) = 0, ||\boldsymbol{w}||_2 \le 1$.

Lemma 2[12]**.** Given a matrix $Q \in \mathbf{R}^{n\times n}, Q > 0$, and a real positive number γ, let $V(\boldsymbol{x}) = \boldsymbol{x}^{\mathrm{T}}Q^{-1}\boldsymbol{x}$. For system (7), if there exist a matrix $Y \in \mathbf{R}^{m\times n}$ and a diagonal matrix $U > 0$ satisfying (1) and

$$\mathrm{He}\begin{bmatrix} AQ & B_w & 0 & B_qU \\ 0 & -I/2 & 0 & 0 \\ C_zQ & D_{zw} & -\gamma^2 I/2 & D_{zq}U \\ C_yQ - Y & D_{yw} & 0 & -U + D_{yq}U \end{bmatrix} \le 0 \tag{10}$$

then the same conclusion as in Lemma 1 can be drawn.

Remark 1. Based on the polytopic differential inclusions instead of the norm-bounded differential inclusions, the condition of Lemma 1 is less conservative than that of Lemma 2, at the cost of introducing more LMIs and thus bringing a higher computational complexity. So the system synthesis tools induced from Lemma 1 are intrinsically less conservative.

Theorem 1. Given a matrix $Q \in \mathbf{R}^{n\times n}, Q > 0$, and real positive numbers ϵ and γ, we assume that $F\boldsymbol{q}$ does not enter the controller output equation, namely, the lower part of the anti-windup gain matrix $F \in \mathbf{R}^{(n_c+m)\times 2m}$ is $0_{m\times 2m}$. For the augmented system (5) and (6) with the closed-loop interconnection as shown in Fig. 1, if there exist matrices $Y, G \in \mathbf{R}^{m\times n}$, $G = C_yQ - Y$ satisfying (1) and (11), then $\mathcal{E}(Q^{-1})$ is a contractively invariant ellipsoid with $\boldsymbol{w} = 0$ and $||\boldsymbol{z}||_2 \le \gamma||\boldsymbol{w}||_2$ for $\boldsymbol{x}(0) = 0, ||\boldsymbol{w}||_2 \le 1$.

$$\mathrm{He}\begin{bmatrix} AQ & B_w + (B_1 + B_2F)\Delta_iD_{yw} & 0 & B_1 + B_2F & 0 \\ 0 & -I/2 & 0 & 0 & 0 \\ C_zQ + Z_1\Delta_iG & D_{zw} + Z_1\Delta_iD_{yw} & -\gamma^2 I/2 & 0 & 0 \\ 0 & 0 & 0 & -\epsilon/2 & 0 \\ G & 0 & 0 & 0 & -1/(2\epsilon) \end{bmatrix} \le 0 \tag{11}$$

Proof. Under the assumption

$$F \in \left\{ \begin{bmatrix} F_1 \\ 0_{m\times 2m} \end{bmatrix} \middle| \quad F_1 \in \mathbf{R}^{n_c\times 2m} \right\}$$

simple calculation shows that $D_{yq} = 0$ and $D_{zq} = Z_1$ are definite matrices. We can argue that the algebraic loop of the system is well-posed, since D_{yq} certainly satisfies a well-posedness equivalent condition that the values of $\det(I - D_{yq}\Delta_i)$ are all nonzero and have the same sign[12].

Noting that $T_i = \Delta_i$, we have the condition in Lemma 1 as follows

$$\text{He}\begin{bmatrix} AQ + B_q\Delta_i G & B_w + B_q\Delta_i D_{yw} & 0 \\ 0 & -I/2 & 0 \\ C_zQ + D_{zq}\Delta_i G & D_{zw} + D_{zq}\Delta_i D_{yw} & -\gamma^2 I/2 \end{bmatrix} \le 0 \tag{12}$$

where $G = C_yQ - Y$. Recall the well known fact that if

$$\epsilon DD^{\rm T} + \epsilon^{-1}E^{\rm T}E < 0$$

is feasible for some real number $\epsilon > 0$, then $D\Delta E + (D\Delta E)^{\rm T} < 0$ holds for all matrices Δ satisfying $\Delta^{\rm T}\Delta \le I$. By applying the above fact and the Schur complements, we get (11) which is a sufficient condition of (12). The proof ends finally from Lemma 1. □

Remark 2. Since (11) is not an LMI, we actually implement an iterative LMI optimization procedure with two steps. First, solve the following LMI with a randomly presetted $\epsilon > 0$, then start the new iteration by choosing a new ϵ according to the norms of B_q and G. In general, the procedure does not guarantee a global or even local optimum. However, better results can be expected in conjunction with some other heuristic optimization algorithms.

$$\begin{aligned} \min_{Q>0,F,G} \quad & \gamma^2 \\ \text{s.t.} \quad & (11) \quad \text{and} \\ & (1) \quad \text{with} \quad Y = C_yQ - G \end{aligned} \tag{13}$$

Theorem 2. Given a matrix $Q > 0$ and a real number $\gamma > 0$, if there exist matrices $Y \in \mathbf{R}^{m\times n}, M \in \mathbf{R}^{(n_c+m)\times 2m}$, and a diagonal matrix $U > 0$ satisfying (1) and the following LMI, then $\mathcal{E}(Q^{-1})$ is a contractively invariant ellipsoid with $\boldsymbol{w} = 0$ and $||\boldsymbol{z}||_2 \le \gamma||\boldsymbol{w}||_2$ for $\boldsymbol{x}(0) = 0, ||\boldsymbol{w}||_2 \le 1$. In addition, the static anti-windup gain F is given by MU^{-1}.

$$\text{He}\begin{bmatrix} AQ & B_w & 0 & B_1U + B_2M \\ 0 & -I/2 & 0 & 0 \\ C_zQ & D_{zw} & -\gamma^2 I/2 & Z_1U + Z_2M \\ C_yQ - Y & D_{yw} & 0 & -U + Y_1U + Y_2M \end{bmatrix} \le 0 \tag{14}$$

Proof. The LMI condition (14) stems directly from the condition (10) of Lemma 2 by substituting $FU = M$ and recalling from above that $B_q = B_1 + B_2F$, $D_{yq} = Y_1 + Y_2F$, and $D_{zq} = Z_1 + Z_2F$. Then, according to Lemma 2, we completes the proof. □

3 Numerical example

Consider the system (2) and (3) with the parameters

$$A_p = \begin{bmatrix} 0 & 1 \\ -2 & 0 \end{bmatrix}, \quad \boldsymbol{B}_{pu} = \begin{bmatrix} 0.1 \\ -1 \end{bmatrix}, \quad \boldsymbol{B}_{pw} = \begin{bmatrix} 1 \\ 0 \end{bmatrix}$$

$$\boldsymbol{C}_{py} = \begin{bmatrix} 1 & 0 \end{bmatrix}, \quad D_{pyu} = 0.8, \quad D_{pyw} = 1$$

$$C_{pz} = \begin{bmatrix} 1 & 0 \\ 0 & 1 \\ 0 & 0 \end{bmatrix}, \quad \boldsymbol{D}_{pzu} = \begin{bmatrix} 0 \\ 0 \\ 1 \end{bmatrix}, \quad \boldsymbol{D}_{pzw} = \begin{bmatrix} 0 \\ 0 \\ 0 \end{bmatrix}$$

$$K_1 = 1.1, \quad K_2 = -0.5$$

It is easy to see from the above parameters that $||\boldsymbol{z}_p||_2^2 = \int_0^\infty (\boldsymbol{x}_1^2 + \boldsymbol{x}_2^2 + \boldsymbol{u}_p^2){\rm d}t$, which covers the guaranteed cost control problem with quadratic cost function. The parameters of the pre-designed unconstrained controller (4) are listed as:

$$A_c = \begin{bmatrix} -2 & 0 \\ 0 & -1 \end{bmatrix}, \boldsymbol{B}_{cy} = \begin{bmatrix} 1.2 \\ 1 \end{bmatrix}, \boldsymbol{B}_{cw} = \begin{bmatrix} 0 \\ 0 \end{bmatrix}, \boldsymbol{C}_c^{\rm T} = \begin{bmatrix} -1.24 \\ 0 \end{bmatrix}$$

By solving the optimization problem (13), we get a static anti-windup gain as

$$F^* = \begin{bmatrix} 1.350 & 0.499 \\ 0.348 & 0.831 \\ 0 & 0 \end{bmatrix}$$

with $\epsilon^* = 2.89, \gamma^* = 24.957$. While from Theorem 2, we can get another static anti-windup gain as

$$F^* = \begin{bmatrix} 5.227 & 1.926\times 10^{-8} \\ 0.600 & 4.436\times 10^{-9} \\ -0.035 & 0.909 \end{bmatrix}$$

with $U^* = \text{diag}\{0.434, 8.089\times 10^7\}$ and a smaller $\gamma^* = 5.785$, indicating that the second method outperforms the other for this case. But this is not always true since it is hard to theoretically analyze the conservativeness of the two methods.

Subject to an impulse disturbance with unit energy, the state responses starting from zero initial condition are plotted in Fig. 3 for four cases. To justify the effectiveness of the proposed methods, the magnified curves around the peak are also shown in the top left margin. From the dotted and the solid curves, we can see that the unconstrained performance seriously deteriorates when the the actual saturation is considered. The proposed two anti-windup design methods do work in that the dashed and the dash-dot curves keep closer to the solid curve.

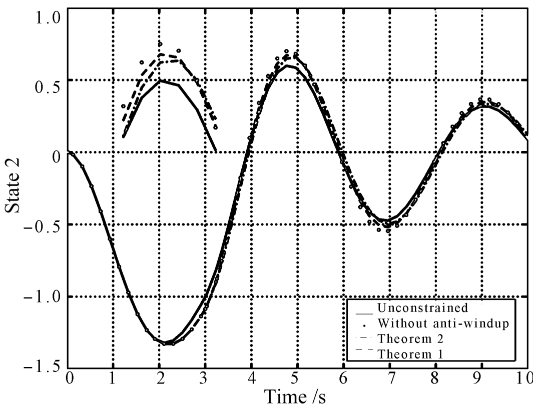

Fig. 3 State responses with and without anti-windup

4 Conclusion

For a certain class of linear saturated systems, an appropriate static anti-windup solution is proposed, as shown in Theorem 1, with guaranteed algebraic loop well-posedness. The problem of well-posedness in Theorem 2 needs further study. Dynamic anti-windup compensator introduces more free parameters in system synthesis and is hence potential in improving the results.

References

1 Chen P C, Shamma J S. Gain-scheduled l^1-optimal control for boiler-turbine dynamics with actuator saturation. *Journal of Process Control*, 2004, **14**(3): 263−277

2 Tzeng C Y, Lin K F. Adaptive ship steering autopilot design with saturating and slew rate limiting actuator. *International Journal of Adaptive Control and Signal Processing*, 2000, **14**(4): 411−426

3 Kapila V, Valluri S. Model predictive control of systems with actuator amplitude and rate saturation. In: Proceedings of the 37th IEEE Conference on Decision and Control. Tampa, USA: IEEE, 1998. 1396−1401

4 Wu F, Soto M. Extended anti-windup control schemes for LTI and LFT systems with actuator saturations. *International Journal of Robust and Nonlinear Control*, 2004, **14**(15): 1255−1281

5 Kapila V, Pan H, De Queiroz M S. LMI-based control of linear systems with actuator amplitude and rate nonlinearities. In: Proceedings of the 38th IEEE Conference on Decision and Control. Phoenix, USA: IEEE, 1999. 1413−1418

6 Grimm G, Postlethwaite I, Teel A R, Turner M C, Zaccarian L. Linear matrix inequalities for full and reduced order anti-windup synthesis. In: Proceedings of the American Control Conference. Arlington, USA: IEEE, 2001. 4134−4139

7 Grimm G, Hatfield J, Postlethwaite I, Teel A R, Turner M C, Zaccarian L. Anti-windup for stable linear systems with input saturation: an LMI-based synthesis. *IEEE Transactions on Automatic Control*, 2003, **48**(9): 1509−1525

8 Galeani S, Onori S, Teel A R, Zaccarian L. A magnitude and rate saturation model and its use in the solution of a static anti-windup problem. *Systems and Control Letters*, 2008, **57**(1): 1−9

9 Hu T S, Lin Z L, Chen B M. An analysis and desing method for linear systems subject to actuator saturation and disturbance. *Automatica*, 2002, **38**(2): 351−359

10 Hu T S, Lin Z L, Chen B M. Analysis and design for linear discrete-time linear systems subject to actuator saturation. *Systems and Control Letters*, 2002, **45**(2): 97−112

11 Hu T S, Lin Z L. Composite quadratic Lyapunov functions for constrained control systems. *IEEE Transactions on Automatic Control*, 2003, **48**(3): 440−450

12 Hu T S, Teel A R, Zaccarian L. Stability and performance for saturated systems via quadratic and nonquadratic Lyapunov functions. *IEEE Transactions on Automatic Control*, 2006, **51**(11): 1770−1786

13 Hu T S, Teel A R, Zaccarian L. Anti-windup synthesis for linear control systems with input saturation: achieving regional, nonlinear performance. *Automatica*, 2008, **44**(2): 512−519

14 Hu T S. Nonlinear control design for linear differential inclusions via convex hull of quadratics. *Automatica*, 2007, **43**(4): 685−692

LIU Sheng Professor at the College of Automation, Harbin Engineering University. His research interest covers intelligent control, robust control, and ship motion control.
E-mail: liu.sch@163.com

ZHOU Li-Ming Ph. D. candidate at the College of Automation, Harbin Engineering University. Her research interest covers constrained control, robust control, and ship steering control. Corresponding author of this paper.
E-mail: zhouliminghit@sohu.com